

# Assessing SAR<sub>1g</sub> Distribution in the Human Head During Hands-Free Mobile Phone Usage

Uglješa Jovanović<sup>1</sup>, Darko Zigar<sup>1</sup>,  
Jelena Malenović-Nikolić<sup>1</sup>, Dejan Krstić<sup>1</sup>

**Abstract:** This paper explores the distribution pattern of SAR<sub>1g</sub> within the adult male head during utilization of hands-free operation of contemporary mobile phones as a source of electromagnetic radiation. The research assesses the optimal positioning of the mobile phone by examining three distinct orientations to determine the minimal SAR<sub>1g</sub> distribution compared to the conventional talking position when hands-free feature is not utilized. The analysis encompasses GSM bands operating at 900 MHz and 1800 MHz, depending on the alignment between the mobile phone and the head.

**Keywords:** Adult male head, SAR<sub>1g</sub>, Electromagnetic radiation, Mobile phone, Simulation.

## 1 Introduction

The classification of electromagnetic radiation (EMR) emitted by mobile phones as a Group 2B possible carcinogen by regulatory bodies, such as the International Agency for Research on Cancer (IARC), has spurred persistent concerns regarding its impact on human health [1, 2]. In response, considerable research efforts have been dedicated to investigating potential associations between EMR exposure and various neurological and cognitive disorders, including headaches, dizziness, memory loss, reduced concentration, and sleep disturbances [3–6].

The proliferation of mobile phones in our daily lives has amplified these concerns, underscoring the urgent need for strategies to mitigate potential health risks. Consequently, manufacturers of contemporary mobile phones often equip them with a hands-free feature, offering users the option to minimize direct contact between the devices and the parts of their body. This feature has garnered

---

<sup>1</sup>University of Niš, Faculty of Occupational Safety Niš, Čarnojevića 10a, 18000 Niš, Serbia;  
E-mails: [ugljesa.jovanovic@zrnrfak.ni.ac.rs](mailto:ugljesa.jovanovic@zrnrfak.ni.ac.rs); [darko.zigar@zrnrfak.ni.ac.rs](mailto:darko.zigar@zrnrfak.ni.ac.rs); [jelena.malenovic@zrnrfak.ni.ac.rs](mailto:jelena.malenovic@zrnrfak.ni.ac.rs);  
[dejan.krstic@zrnrfak.ni.ac.rs](mailto:dejan.krstic@zrnrfak.ni.ac.rs).

\*An earlier version of this paper was presented at the 16<sup>th</sup> International Conference on Applied Electromagnetics - IIEC 2023, August 28 – 30, 2023, in Niš, Serbia.

significant attention, particularly among users with the need to reduce exposure to EMR emitted by mobile phones.

To address these concerns, regulatory agencies have introduced the concept of Specific Absorption Rate (SAR) as a precautionary safety measure. SAR quantifies the rate of EMR absorption over a specified mass of biological tissue and has led to the establishment of SAR limitations. In the United States, the Federal Communications Commission (FCC) mandates that mobile phones must comply with SAR limits not exceeding 1.6 W/kg, averaged over 1 gram of tissue [7], while in Europe, the European Committee for Electrotechnical Standardization (CENELEC) sets the SAR limit at 2 W/kg, averaged over 10 grams of tissue [8]. These regulatory measures aim to mitigate potential health risks associated with mobile phone usage by limiting the absorption of EMR in biological tissues.

However, despite these regulatory efforts, questions persist regarding the dispersion patterns of SAR within the human head, particularly when utilizing hands-free features. Understanding the intricate variations in SAR levels across distinct regions of the head is crucial for assessing potential health risks associated with mobile phone usage.

This research focuses on investigating the dispersion patterns of SAR within the human head when employing the hands-free feature of modern mobile phones. Our inquiry delves into the complex dynamics of SAR distribution across different regions of the head, taking into account the implementation of hands-free functionalities as a potential mitigating factor.

## **2 Simulation Method**

The simulations in this investigation were conducted using CST Studio, a well-established software tool recognized for its proficiency in electromagnetic simulations. Employing the finite integration technique, this software discretizes the integral formulation of Maxwell's equations.

The assessment of EMR absorption within the adult male human head was conducted on the AustinMan 2.6 voxel-based human model. The employed model of the human head, comprising 27 intricately detailed tissues, has demonstrated its efficacy in simulating EMR absorption and has been applied in various pertinent research studies [9 – 11].

To ensure the utmost accuracy in the results, the dielectric properties of biological tissues were acquired from the IT'IS Foundation. These parameters are provided in **Table 1** for both simulated GSM bands [12]. Herein,  $\epsilon_r$  denotes permittivity in [F/m], and  $\sigma$  represents electrical conductivity in [S/m].

In this research, a contemporary mobile phone model from CST Studio served as the EMR source. The mobile phone is equipped with three antennas,

with one operating at 900 MHz and two at 1800 MHz. To maintain consistency with comparable studies, the output power of all antennas was adjusted to 1 W [13]. SAR<sub>1g</sub> distributions were calculated according to the IEEE C95.3 standard.

Analyses were conducted for four of the most common mobile phone positions observed among users. The initial simulation placed the mobile phone in the conventional talking position, serving as the baseline for the remaining three simulations. In these subsequent simulations, the mobile phone was used in hands-free mode. These three positions were chosen to closely replicate the widely adopted orientations in which users, with minor variations, typically engage with mobile phones. Based on the mobile phone's position, the simulation analysis focuses on the dominant antenna(s).

**Table 1**  
*Dielectric properties of head tissues at 900 MHz and 1800 MHz.*

Tissue	900 MHz		1800 MHz	
	$\epsilon_r$	$\sigma$	$\epsilon_r$	$\sigma$
Blood Vessel	44.775	0.696	43.343	1.065
Bone Cortical	12.453	0.143	11.780	0.275
Bone Marrow	5.504	0.040	5.371	0.069
Brain Grey Matter	52.725	0.942	50.079	1.391
Brain White Matter	38.886	0.590	37.011	0.915
Cartilage	42.652	0.782	40.215	1.287
Cerebellum	49.444	1.262	46.114	1.709
Cerebrospinal Fluid	68.638	2.412	67.201	2.923
Dura	44.426	0.961	42.893	1.319
Eye Cornea	55.235	1.394	52.768	1.858
Eye Lens	46.572	0.793	45.353	1.147
Eye Sclera	55.270	1.166	53.568	1.602
Eye Vitreous Humor	68.901	1.636	68.573	2.032
Fat	5.461	0.051	5.349	0.078
Lymph	59.683	1.038	58.142	1.501
Medulla	49.444	1.262	46.114	1.709
Midbrain	49.444	1.262	46.114	1.709
Mucous Membrane	55.031	0.942	53.549	1.341
Muscle	55.031	0.942	53.549	1.341
Nerve	32.530	0.573	30.867	0.843
Pons	49.444	1.262	46.114	1.709
Salivary Gland	75.986	0.815	74.682	0.967
Skin	41.405	0.866	38.872	1.185
Spinal Cord	32.530	0.573	30.867	0.843
Tendon	45.825	0.718	44.251	1.201
Tongue	55.270	0.936	53.568	1.371
Tooth	12.453	0.143	11.780	0.275

### 3 Results

Throughout all simulations, the mobile phone was held in as natural a manner as possible, mimicking the typical grip by a human hand. This approach aimed to ensure a realistic representation of how users commonly hold their mobile phones.

#### 3.1 The first simulated position

As previously indicated, in the initial simulated position, the mobile phone is situated in a traditional talking stance without utilizing the hands-free feature. This involves positioning the mobile phone against the preferred ear and cheekbone. In this particular simulation, the mobile phone is inclined against the right ear and cheekbone, as depicted in Fig. 1, plainly because the antenna operating at 900 MHz exhibits a more pronounced effect on the head tissues compared to the scenario where it is leaned against the left ear and cheekbone.

The red arrows in Fig. 1 signify the positions of all three antennas and the directions of their radiation, with the red numbers serving as designations for antennas operating at 1800 MHz. Fig. 2 illustrates the  $SAR_{1g}$  distribution on the head's surface for the initial simulated position presented in Fig. 1.

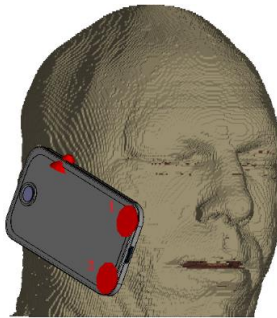


**Fig. 1** – *Conventional talking stance.*

In Fig. 2, the  $SAR_{1g}$  distribution is notably concentrated in the upper region of the cheekbone. Upon initial inspection, the absorption area appears to be quite substantial, and the recorded peak value of 2.878 W/kg significantly exceeds the permissible limit of 1.6 W/kg. This outcome is expected due to the close proximity of the antenna to the head.

The depth of EMR penetration within the head tissues for the  $SAR_{1g}$  distribution depicted in Fig. 2 is clearly illustrated in the cross-sectional view presented in Fig. 3.

It's essential to note that only a fraction of the absorbed EMR effectively reaches the surface of the brain, with the majority being absorbed by the skin, fat tissue and skull bone [11], as Fig. 3 shows. Moreover, a noteworthy amount of EMR is absorbed by the right eye.

The way the mobile phone is held in Fig. 1 highlights the smaller impact of the two antennas operating at 1800 MHz compared to the antenna operating at 900 MHz. Fig. 4 displays SAR<sub>1g</sub> distributions on the surface of the head for both antennas operating at 1800 MHz in the standard talking stance.

Both SAR<sub>1g</sub> distributions affect the same tissues as SAR<sub>1g</sub> distribution shown in Fig 2 but with considerably lower values especially in the case of the antenna 2. The recorded peak values are 1.532 W/kg for antenna 1 and 0.887 W/kg for antenna 2.

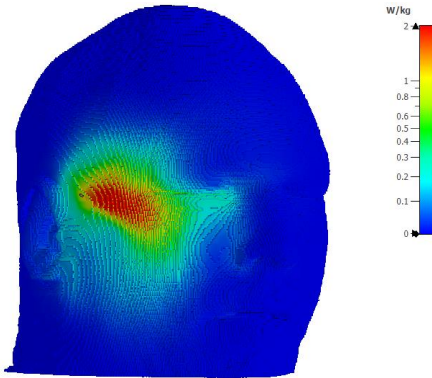


**Fig. 2** – Distribution of SAR<sub>1g</sub> in the conventional talking stance.

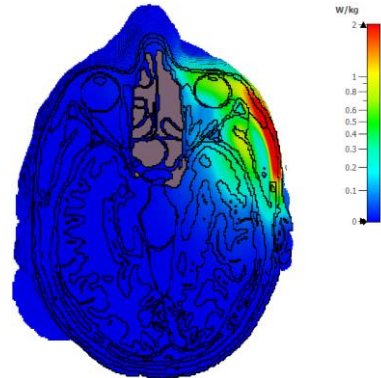
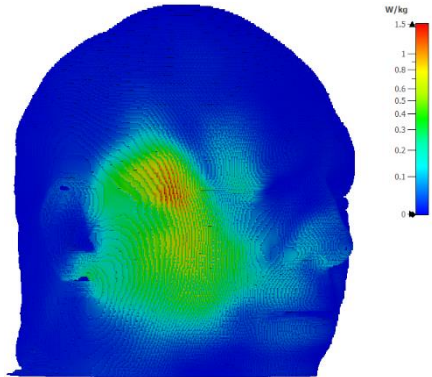
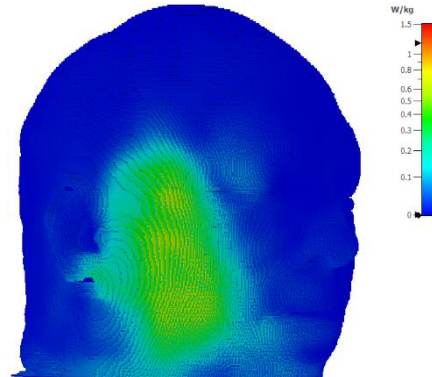


**Fig. 3** – Cross-sectional view of SAR<sub>1g</sub> distribution within the head.



(a)



(b)

**Fig. 4** – Distribution of SAR<sub>1g</sub> originating from: (a) antenna 1; (b) antenna 2.

Fig. 5 provides a cross-sectional view of the SAR<sub>1g</sub> distribution within the head, highlighting the affected tissues.

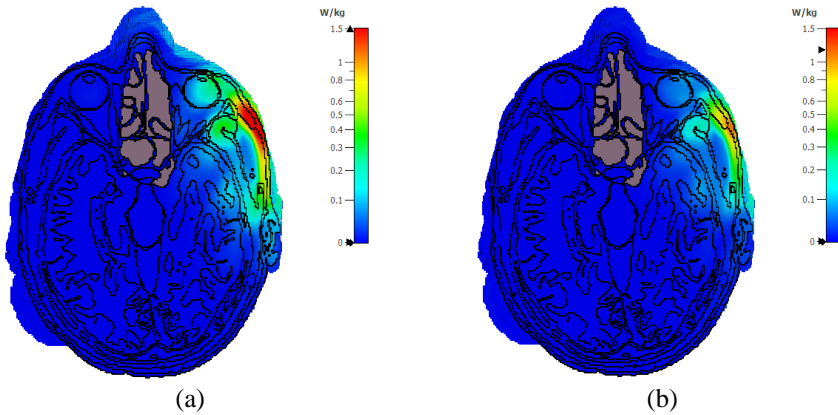


**Fig. 5** – Cross-sectional view of  $SAR_{1g}$  distribution originating from: (a) antenna 1; (b) antenna 2.

Both distributions are quite similar, with the difference being that antenna 2 has a slightly lesser impact on tissues, as reflected in the lower  $SAR_{1g}$  values.

### 3.2 The second simulated position

In the second simulated position, the mobile phone is positioned on the left side of the head, parallel to the ground, with its side edge resting opposite to the cheekbone, as depicted in Fig. 6.

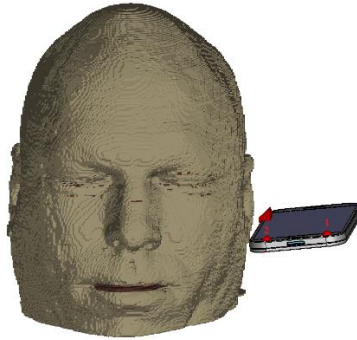
The red numbers in Fig. 6 serve as designations for antennas operating at 1800 MHz. In this configuration, the mobile phone's microphone is positioned near the mouth, and there is a gap of approximately 2 cm between the head and the mobile phone, equivalent to the typical thickness of a human thumb. Placing the mobile phone on the left side of the head aligns the antenna, operating at 900 MHz, toward the head, resulting in increased absorption of EMR and, consequently,  $SAR_{1g}$ , representing a worst-case scenario for the user.

Fig. 7 illustrates the  $SAR_{1g}$  distribution across the head's surface for the antenna operating at 900 MHz, with the alignment as shown in Fig. 6.

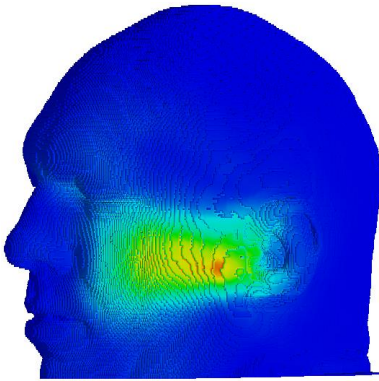
While the antenna emits EMR directly toward the head, the  $SAR_{1g}$  distribution reveals that only a portion of the emitted EMR is absorbed by the head tissues. The recorded peak value of 0.8526 W/kg is roughly at half the permissible limit, thus well within the safety threshold.

Fig. 8 presents a cross-sectional view of the  $SAR_{1g}$  distribution within the head, highlighting the affected tissues.

The cross-sectional view of  $SAR_{1g}$  distribution reveals that EMR absorption primarily occurs within fat tissue, bones, muscles, and the salivary gland, with negligible absorption within the brain.



**Fig. 6** – *The alignment between the head and the mobile phone in the second position.*



**Fig. 7** – *Distribution of SAR<sub>1g</sub> in the second position.*

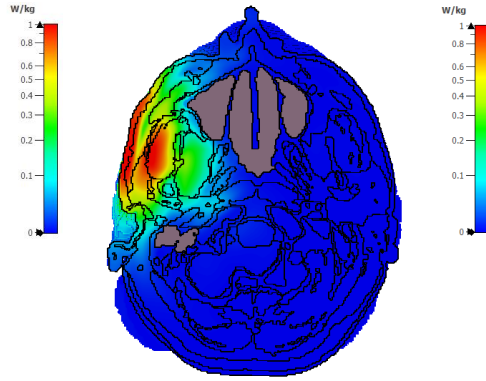
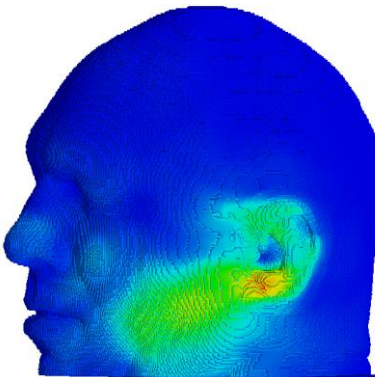
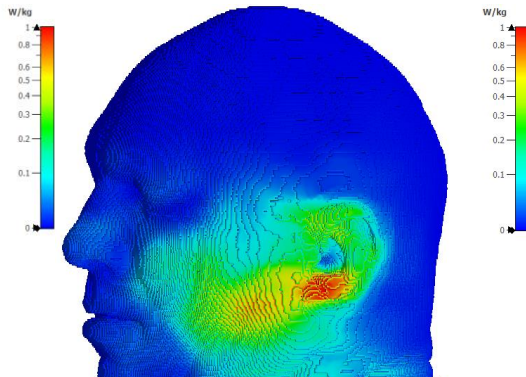


**Fig. 8** – *Cross-sectional view of SAR<sub>1g</sub> distribution within the head.*



(a)



(b)

**Fig. 9** – *Distribution of SAR<sub>1g</sub> originating from: (a) antenna 1; (b) antenna 2.*

Fig. 9 illustrates SAR<sub>1g</sub> distributions on the head's surface for both antennas operating at 1800 MHz when the mobile phone is held as depicted in Fig. 6.

The SAR<sub>1g</sub> distributions for both antennas exhibit higher values compared to SAR<sub>1g</sub> distribution shown in Fig. 7. Specifically, the maximal recorded values are 0.992 W/kg for antenna 1 and 1.254 W/kg for antenna 2, both within the permissible limit.

Fig. 10 provides a cross-sectional view of the SAR<sub>1g</sub> distribution within the head, highlighting the affected tissues.

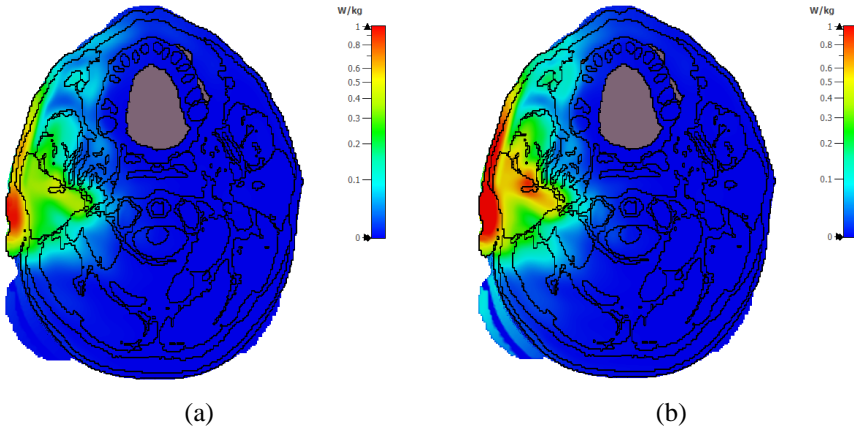


**Fig. 10** – Cross-sectional view of SAR<sub>1g</sub> distribution originating from: (a) antenna 1; (b) antenna 2.

Based on both SAR<sub>1g</sub> distributions, it can be concluded that EMR absorption still primarily occurs within fat tissue, bones, muscles, cartilage, and the salivary gland, with minimal absorption within the brain and eyes. Notably, EMR emitted by antenna 2 penetrates deeper into the tissues due to its closer proximity to the head. Considering that the maximum SAR<sub>1g</sub> value is below the permissible limit, it is a valid and secure conclusion that this position is safer when compared to the first simulated position.

### 3.3 The third simulated position

In the third simulated position, the mobile phone is positioned in front of the face, parallel with the ground, with its screen facing the face and the microphone situated 3 cm ahead of the mouth, as illustrated in Fig. 11.

In this position, only the two antennas operating at 1800 MHz generate a noticeable SAR<sub>1g</sub> distribution on the head, while the antenna operating at 900 MHz has no discernible impact. Therefore, the antenna operating at 900 MHz was excluded from the analysis. The red numbers in Fig. 11 serve as designations for antennas operating at 1800 MHz.

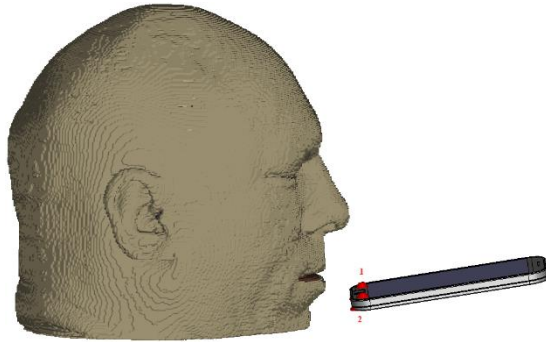


**Fig. 11** – The alignment between the head and the mobile phone in the third position.

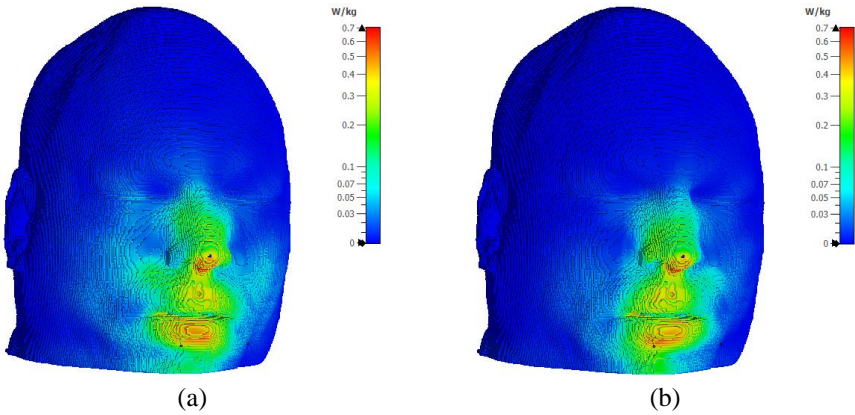


**Fig. 12** – Distribution of SAR<sub>1g</sub> originating from: (a) antenna 1; (b) antenna 2.

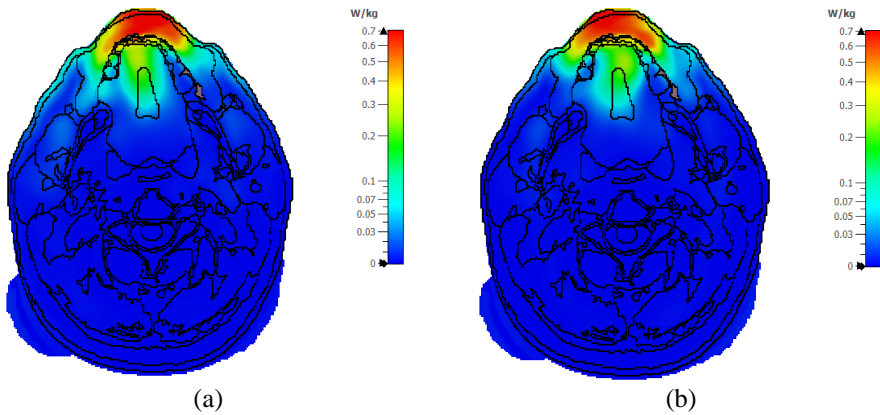


**Fig. 13**– Cross-sectional view of SAR<sub>1g</sub> distribution originating from: (a) antenna 1; (b) antenna 2.

Fig. 12 illustrates SAR<sub>1g</sub> distributions on the head's surface for both antennas when the mobile phone is held as illustrated in Fig. 11.

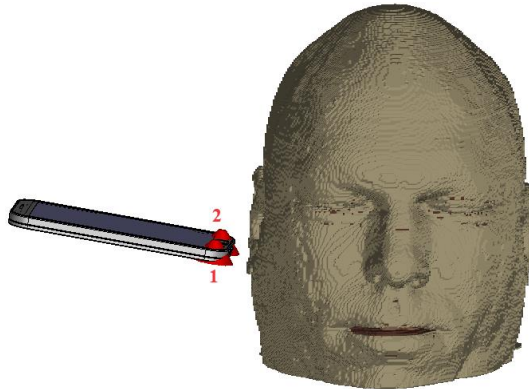
The SAR<sub>1g</sub> distributions for both antennas exhibit remarkable similarity, as expected due to their close proximity. Notably, the maximum levels depicted in both distributions are substantially lower than the permissible limit, with recorded maximal values of 0.838 W/kg for antenna 1 and 0.915 W/kg for antenna 2. It is noteworthy that these values are comparable to the previous simulated position.

Fig. 13 displays the cross-sectional views of both SAR<sub>1g</sub> distributions and the tissues that absorb the EMR.

Based on Figs. 12 and 13, the most notable SAR<sub>1g</sub> levels are concentrated at the tip of the nose and in the region between the lower lip and chin. In addition, the EMR emitted by both antennas is almost entirely absorbed by the fat tissue and the frontal teeth of both jaws, with only a marginal portion reaching the ocular region.

### 3.4 The fourth simulated position

In the fourth simulation, the mobile phone is situated parallel to the ground with its screen facing the ear, and the microphone is positioned 2 cm away from the ear, as illustrated in Fig. 14. The red numbers in Fig. 14 serve as designations for antennas operating at 1800 MHz.



**Fig. 14** – *The alignment between the head and the mobile phone in the fourth position.*

In this scenario, the orientation of the mobile phone, whether directed towards the right or left ear, does not yield any differentiation. Regarding the position of the mobile phone, only both antennas operating at 1800 MHz were analyzed in this scenario since the antenna operating at 900 MHz doesn't produce any notable effect. Therefore, the SAR<sub>1g</sub> distributions depicted in Fig. 15 correspond to this specific frequency range and positioning of the device.

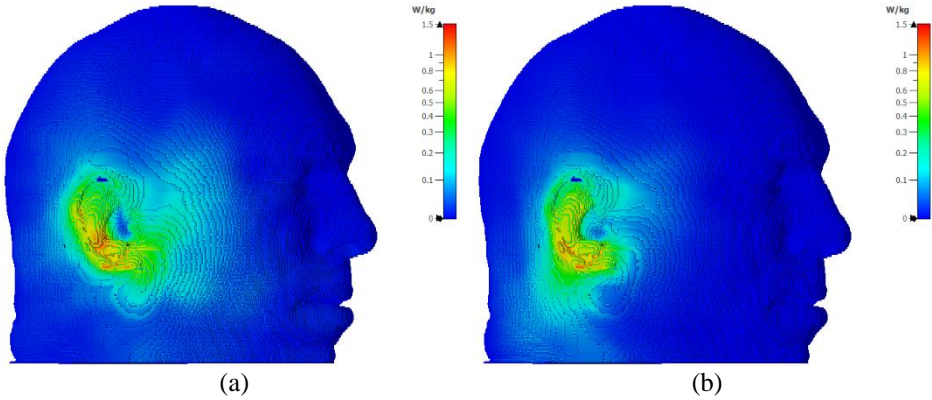


**Fig. 15** – Distribution of SAR<sub>1g</sub> originating from: (a) antenna 1; (b) antenna 2.

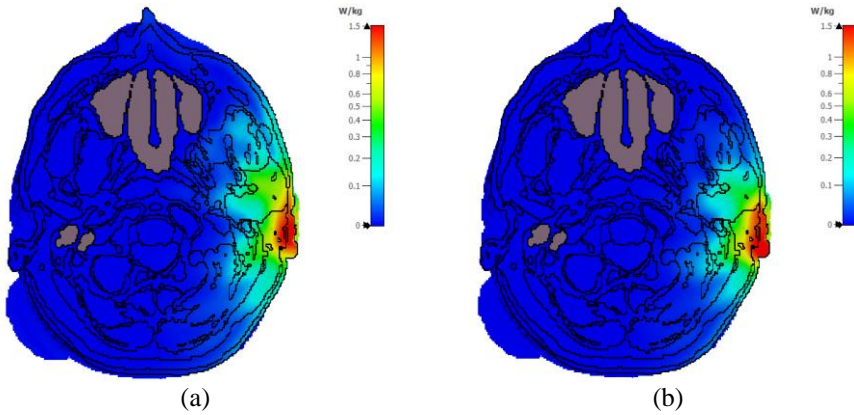


**Fig. 16** – Cross-sectional view of SAR<sub>1g</sub> distribution originating from: (a) antenna 1; (b) antenna 2.

Similar to the previous simulation, both SAR<sub>1g</sub> distributions exhibit a significant degree of similarity. However, these SAR<sub>1g</sub> distributions display higher values compared to the previous simulated position. Specifically, the maximal recorded value for antenna 1 is 1.468 W/kg, while for antenna 2, it is 1.387 W/kg. Although these values are in close proximity to the permissible limit, the absorbed EMR is primarily focused on the ear shell, fat tissues, muscles and salivary gland as can be seen on cross-sectional views of both SAR<sub>1g</sub> distributions shown in Fig. 16.

It's important to note that a minor part of the EMR is absorbed by the brain because the absorption rate depends on the proximity between the mobile phone and the head, as well as the tilt angle of the mobile phone.

## **4 Conclusion**

This study has provided an analysis of SAR<sub>1g</sub> distribution across the adult male head arising from the EMR emitted by contemporary mobile phone. Specifically, three prevalent positions of mobile phone use with hands-free features were examined, with the conventional talking stance serving as the reference point.

The findings from this analysis are consistent and noteworthy. Notably, SAR<sub>1g</sub> levels observed in all simulations involving hands-free feature usage consistently remained below the established maximum permissible value. In contrast, SAR<sub>1g</sub> level associated with the conventional talking stance exceeded the permissible threshold. These results undeniably emphasize the effectiveness of the hands-free feature in achieving one of its primary objectives: mitigating human exposure to the EMR emitted by mobile phones.

A considerable number of mobile phone users are often unaware of the precise locations of the antennas within their devices, which can occasionally be concerning, as demonstrated in this research. A potential remedy for this issue involves periodically alternating the placement of the mobile phone between ears. This practice allows blood circulation to cool down the affected tissues, effectively mitigating potential concerns.

In conclusion, this research emphasizes the crucial role of the hands-free feature in mitigating potential health risks associated with mobile phone usage. By maintaining SAR<sub>1g</sub> levels within safe limits, this technology showcases its ability to protect human well-being in the context of the EMR exposure. The study provides valuable insights for both users and manufacturers, highlighting the significance of ongoing advancements in mobile phone technology to ensure safer interactions with these devices.

## **5 Acknowledgments**

The research presented in this paper is funded by the Ministry of Science of the Republic of Serbia under the grant 451-03-66/2024-03/200148.

## **6 References**

- [1] U. Jovanović, D. Zigar, J. Malenović-Nikolić, D. Krstić: Distribution of SAR<sub>1g</sub> in a Human Head when Using a Mobile Phone with the Hands-Free Feature, Proceedings of the 16<sup>th</sup> International Conference on Applied Electromagnetics - IIEC 2023, Niš, Serbia, August 2023, pp. 54–57.
- [2] R. Baan, Y. Grosse, B. Lauby-Secretan, F. El Ghissassi, V. Bouvard, L. Benbrahim-Tallaa, N. Guha, F. Islami, L. Galichet, K. Straif: Carcinogenicity of Radiofrequency Electromagnetic Fields, *The Lancet Oncology*, Vol. 12, No. 7, July 2011, pp. 624–626.
- [3] A.H. Frey: Headaches from Cellular Telephones: Are They Real and What are the Implications?, *Environmental Health Perspectives*, Vol. 106, No. 3, March 1998, pp. 101–103.

- [4] H. Danker-Hopfe, H. Dorn, T. Bolz, A. Peter, M.-L. Hansen, T. Eggert, C. Sauter: Effects of Mobile Phone Exposure (GSM 900 and WCDMA/UMTS) on Polysomnography Based Sleep Quality: An Intra-and Inter-Individual Perspective, *Environmental Research*, Vol. 145, February 2016, pp. 50–60.
- [5] H.- P. Hutter, H. Moshammer, P. Wallner, M. Kundi: Subjective Symptoms, Sleeping Problems, and Cognitive Performance in Subjects Living Near Mobile Phone Base Stations, *Occupational and Environmental Medicine*, Vol. 63, No. 5, May 2006, pp. 307–313.
- [6] G. Abdel-Rassoul, O. Abou El-Fateh, M. Abou Salem, A. Michael, F. Farahat, M. El-Batanouny, E. Salem: Neurobehavioral Effects Among Inhabitants around Mobile Phone Base Stations, *Neurotoxicology*, Vol. 28, No. 2, March 2007, pp. 434–440.
- [7] Federal Communications Commission: Specific Absorption Rate (SAR) for Cellular Telephones, Available at: <https://www.fcc.gov/general/specific-absorption-rate-sar-cellular-telephones>.
- [8] IEC/IEEE 62209-1528:2020: Measurement procedure for the assessment of specific absorption rate of human exposure to radio frequency fields from hand-held and body-mounted wireless communication devices – Part 1528: Human models, instrumentation, and procedures (Frequency range of 4 MHz to 10 GHz), 2020.
- [9] J. Massey, C. Geyik, N. Techachainiran, C.-L. Hsu, R. Nguyen, T. Latson, M. Ball, E. Celik, A. Yilmaz: AustinMan and AustinWoman: High Fidelity, Reproducible, and Open-Source Electromagnetic Voxel Models, *Proceedings of the 34<sup>th</sup> Annual Meeting of the Bioelectromagnetics Society*, Brisbane, Australia, June 2012.
- [10] J.W. Massey, A.E. Yilmaz: AustinMan and AustinWoman: High-Fidelity, Anatomical Voxel Models Developed from the VHP Color Images, *Proceedings of the 38<sup>th</sup> Annual International Conference of the IEEE Engineering in Medicine and Biology Society (EMBC)*, Orlando, USA, August 2016, pp. 3346–3349.
- [11] U.Z. Jovanović, D.D. Krstić, D.N. Zigar, J.R. Malenović-Nikolić, S.G. Cvetanović: Temperature Elevation of a Human Brain Induced by a Mobile Phone Electromagnetic Radiation, *Thermal Science*, Vol. 27, No. 3B, November 2023, pp. 2433–2442.
- [12] P.A. Hasgall, F.Di Gennaro, C. Baumgartner, E. Neufeld, B. Lloyd, M.-C. Gosselin, D. Payne, A. Klingenböck, N. Kuster: IT'IS Database for Thermal and Electromagnetic Parameters of Biological Tissues, Version 4.1, 2022, Available at: <https://itis.swiss/virtual-population/tissue-properties/overview/>
- [13] IEC/IEEE 62704-4:2020: Determining the peak spatial-average specific absorption rate (SAR) in the human body from wireless communication devices, 30 MHz to 6 GHz – Part 4: General requirements for using the finite element method for SAR calculations, 2020.